



<b>Publication Year</b>	2020
<b>Acceptance in OA @INAF</b>	2022-02-10T15:50:12Z
<b>Title</b>	First Results on the Experimental Validation of the SKA-low Prototypes Deployed in Australia Using an Airborne Test Source
<b>Authors</b>	Paonessa F.; Ciorba L.; Virone G.; BOLLI, Pietro; Magro A.; et al.
<b>DOI</b>	10.23919/URSIGASS49373.2020.9232190
<b>Handle</b>	<a href="http://hdl.handle.net/20.500.12386/31380">http://hdl.handle.net/20.500.12386/31380</a>
<b>Journal</b>	...URSI GENERAL ASSEMBLY AND SCIENTIFIC SYMPOSIUM

## First Results on the Experimental Validation of the SKA-low Prototypes Deployed in Australia Using an Airborne Test Source

Fabio Paonessa<sup>\*(1)</sup>, Lorenzo Ciorba<sup>(1)</sup>, Giuseppe Virone<sup>(1)</sup>, Pietro Bolli<sup>(2)</sup>, Alessio Magro<sup>(3)</sup>, Andrew McPhail<sup>(4)</sup>, Dave Minchin<sup>(4)</sup>, and Raunaq Bhushan<sup>(4)</sup>

(1) National Research Council of Italy (CNR - IEIIT), Turin, Italy

(2) Italian National Institute for Astrophysics (INAF - OAA), Arcetri, Italy

(3) Institute of Space Sciences and Astronomy, University of Malta, Msida, Malta

(4) International Centre for Radio Astronomy Research (ICRAR), Perth, Australia

### Abstract

As the Square Kilometre Array progresses toward the construction phase, the first prototypes of the low-frequency instrument have been deployed in Australia. To support such a crucial phase, a measurement campaign took place in the Murchison Radio-astronomy Observatory area in order to validate the electromagnetic models of the arrays by characterizing the embedded-element patterns and the array beams. A set of significant results is shown in this contribution.

### 1 Introduction

The future Square Kilometre Array (SKA) [0] radio telescope is approaching the final stage of its development. Within the bridging phase of the low-frequency instrument (SKA-low) [2], which will operate from 50 to 350 MHz, two stations have been built in the Murchison Radio-astronomy Observatory (MRO) area in Western Australia (see Figs. 1 and 2). Both the stations share a random array layout of 256 dual-polarized antennas mounted on a ground plane with a diameter of about 40 m. The Aperture Array Verification System 2.0 (AAVS2.0) station is composed of log-periodic SKALA4.1-AL antennas [3], whereas the Engineering Development Array 2 (EDA2) [4] station is composed of bow-tie antennas already used in the Murchison Widefield Array (MWA) [5].

The accuracy of the electromagnetic models is a critical aspect for such advanced instruments. The embedded element patterns (EEPs) can present significant distortions with respect to the expected behavior [6]. In June 2019, a measurement campaign was carried out at MRO with the main purpose of validating the electromagnetic models of both arrays through an experimental measurement of the EEPs and the digitally beam-formed array patterns exploiting a radio-frequency test source mounted on a small unmanned aircraft. The measurements directly involved research institutions from Italy, Australia and Malta. Before this campaign, the Italian team conducted several activities on low frequency aperture arrays, including the instrumental calibration [7-9] and near-field verification strategies [10, 11]. This contribution shows the relevant results of the MRO campaign.

### 2 Experimental Setup

When the MRO campaign was carried out, 48 antennas out of 256 were deployed in 3 clusters of 16 antennas for AAVS2.0, for this reason its name was AAVS1.5 [12]. EDA2 was fully deployed but only 48 antennas were connected to the receiver. The arrays shared nearly the same configuration. In particular, the layout of AAVS1.5 (illustration in Fig. 3) is slightly enlarged with respect to



**Figure 1.** Aerial view of the AAVS1.5 and EDA2 stations at the MRO site. Picture from <https://virtualtours-external.csiro.au/MRO/>

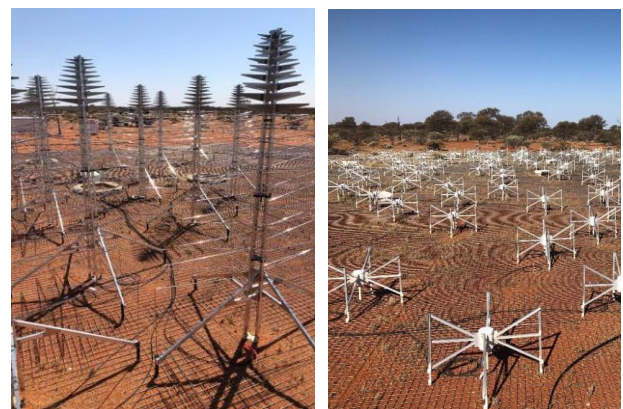


**Figure 2.** The AAVS1.5 SKALA4.1-AL antennas (left) and the EDA2 bow-tie dipoles (right).

EDA2 to accommodate the larger footprint of the elements. The resulting station diameter is 40 m for AAVS1.5 and 35 m for EDA2.

The measurements at MRO have been carried out by using the Unmanned Aerial Vehicle (UAV) system already adopted in [13], [14]. A small multicopter equipped with a Real Time Kinematic (RTK) differential GPS and a tunable radio-frequency generator operated as a flying test source.

The measurements have been performed at the frequencies of 50, 70, 110, 160, 230 and 320 MHz. They consisted in linear scans at a constant height of 120 m or 160 m to characterize the principal cuts of the radiation patterns with an angular coverage of  $\pm 45^\circ$  from zenith [15]. Although at such flying height the test source was not in the far-field of the whole array (considering the three deployed clusters), the far-field condition was satisfied at the embedded-element level.

### 3 Results

Although a relatively small subset of antennas was deployed when the campaign took place, more than 10 GB of data have been collected in two days, corresponding to 14 flights, despite the weather conditions characterized by frequent wind gusts at 40 km/h.

In Fig. 4, the EEPs of two antennas (#0 and #2 of cluster #0) at two different frequencies are shown for the AAVS1.5 station. Antenna #0 is located at the edge of the cluster whereas #2 is closer to other adjacent antennas. Fig. 5 shows the results for the corresponding antennas in the EDA2 station. As previously mentioned, both the arrays share the same layout. We generally observe a good agreement between measurements (blue curves) and simulations (red curves). Similar agreement levels have been obtained for the other 46 elements, a detailed statistical analysis will be shown at the conference.

Figs. 6 and 7 show the normalized beam-formed pattern of cluster #0 (16 antennas) of AAVS1.5 and EDA2, respectively. As expected, the results are rather similar to each other, even though some elements present different behavior. The measured array pattern (blue) has been obtained by equalizing the complex EEPs at the zenith of the cluster. This corresponds to a near-field focusing. The simulations (red) are instead performed in far-field using the Method of Moments (MoM) of Galileo-EMT. The good agreement confirms the effectiveness of near-field focusing for array testing [16].

### 4 Conclusion

This first measurement campaign in Western Australia using a UAV-mounted test source has been conceived to support the deployment the SKA-low prototypes and verify the array models. Further activities will concern the whole 256-elements stations both in terms of the pattern characterization (also adopting near-field strategies) and the evaluation of the instrument performance (e.g. sensitivity).

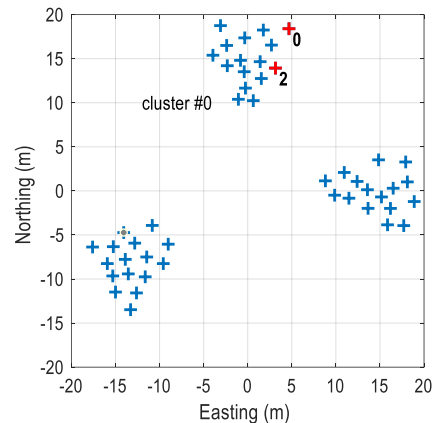


**Figure 3.** Layout of AAVS1.5. Antennas #0 and #2 of cluster #0 highlighted.

### 5 Acknowledgement

The authors thank Gianni Comoretto, Jader Monari, Federico Perini, Simone Rusticelli, Paola Di Ninni (INAF), Daniel Ung, David Davidson (ICRAR), Mirko Bercigli (IDS Corp.), Mark Waterson and André van Es (SKA Office)

### 6 References

1. P. E. Dewdney, P. J. Hall, R. T. Schilizzi and T. J. L. W. Lazio, "The Square Kilometre Array," in Proceedings of the IEEE, vol. 97, no. 8, pp. 1482-1496, Aug. 2009. doi: 10.1109/JPROC.2009.2021005
2. P. Benthem et al., "The low frequency receivers for SKA 1-low: Design and verification," XXXIInd General Assembly and Scientific Symposium of the International Union of Radio Science (URSI GASS), Montreal, QC, 2017, pp. 1-4. doi: 10.23919/URSIGASS.2017.8104992
3. P. Di Ninni, M. Bercigli, P. Bolli, G. Virone and S. J. Wijnholds, "Mutual Coupling Analysis for a SKA1-LOW Station," 13th European Conference on Antennas and Propagation (EuCAP), Krakow, Poland, 2019, pp. 1-5.
4. R. Wayth et al., "The Engineering Development Array: A Low Frequency Radio Telescope Utilising SKA Precursor Technology," Publications of the Astronomical Society of Australia, 34, E034, 2017. doi:10.1017/pasa.2017.27
5. S. Tingay et al., "The Murchison Widefield Array: The Square Kilometre Array Precursor at Low Radio Frequencies," Publications of the Astronomical Society of Australia, 30, E007, 2013. doi:10.1017/pasa.2012.007
6. G. Virone et al., "Strong Mutual Coupling Effects on LOFAR: Modeling and In Situ Validation," in IEEE Transactions on Antennas and Propagation, vol. 66, no. 5, pp. 2581-2588, May 2018. doi: 10.1109/TAP.2018.2816651

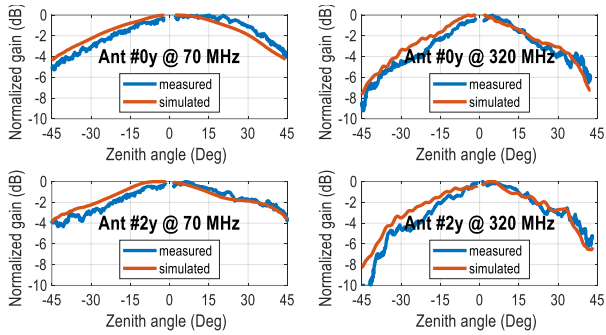


**Figure 4.** Normalized embedded-element patterns of antenna #0 (upper row) and #2 (lower row) of AAVS1.5 (north-south polarization, cluster #0) at 70 MHz (left column) and 320 MHz (right column). Blue: measurements, red: simulations.

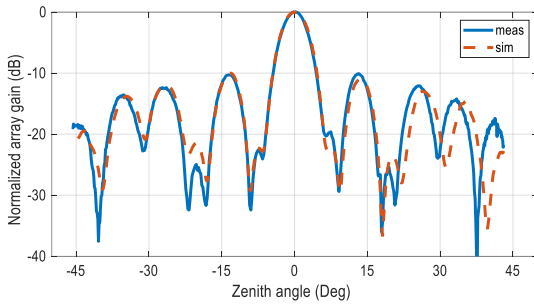


**Figure 6.** Normalized beam-formed pattern of cluster #0 of AAVS1.5 at 320 MHz. Blue: measurements, red: simulations.

7. P. Bolli et al., “In-situ characterization of international low-frequency aperture arrays by means of an UAV-based system,” XXXII General Assembly and Scientific Symposium of the International Union of Radio Science (URSI GASS), Montreal, QC, 2017, pp. 1-4. doi: 10.23919/URSIGASS.2017.8105020

8. E. de Lera Acedo et al., “SKA Aperture Array Verification System: Electromagnetic modeling and beam pattern measurements using a micro UAV”, *Experimental Astronomy*, vol. 45, issue 1, pp. 1–20, Mar. 2018. DOI: 10.1007/s10686-017-9566-x

9. Di Ninni et al., “Electromagnetic analysis and experimental validation of the LOFAR radiation patterns,” *International Journal of Antennas and Propagation*, 2019, art. no. 9191580. doi: 10.1155/2019/9191580

10. P. Bolli, G. Pupillo, F. Paonessa, G. Virone, S. J. Wijnholds and A. M. Lingua, “Near-Field Experimental Verification of the EM Models for the LOFAR Radio Telescope,” in *IEEE Antennas and Wireless Propagation Letters*, vol. 17, no. 4, pp. 613-616, April 2018. doi: 10.1109/LAWP.2018.2805999

11. L. Ciorba et al., “Near-Field Phase Reconstruction for UAV-based Antenna Measurements,” 13th European Conference on Antennas and Propagation (EuCAP), Krakow, Poland, 2019, pp. 1-4.

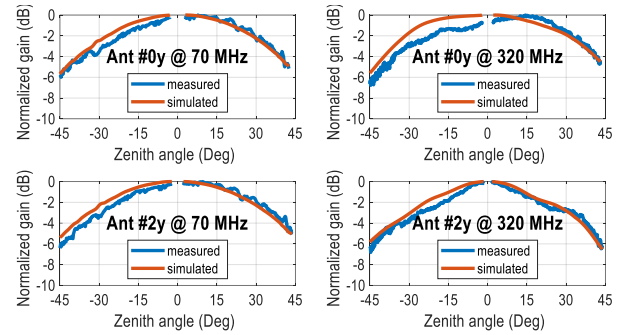


**Figure 5.** Normalized embedded-element patterns of antenna #0 (upper row) and #2 (lower row) of EDA2 (north-south polarization, cluster #0) at 70 MHz (left column) and 320 MHz (right column). Blue: measurements, red: simulations.

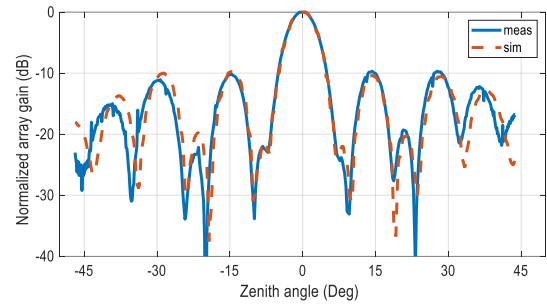


**Figure 4.** Normalized beam-formed pattern of cluster #0 of EDA2 at 320 MHz. Blue: measurements, red: simulations.

12. D. B. Davidson et al., “Electromagnetic modelling of the SKA-LOW AAVS1.5 prototype,” *International Conference on Electromagnetics in Advanced Applications (ICEAA)*, Granada, Spain, 2019, pp. 1032-1037. doi: 10.1109/ICEAA.2019.8879294

13. F. Paonessa et al., “Characterization of the Murchison Widefield Array Dipole with a UAV-mounted Test Source,” 13th European Conference on Antennas and Propagation (EuCAP), Krakow, Poland, 2019, pp. 1-4.

14. F. Paonessa, G. Virone, P. Bolli, G. Addamo, S. Matteoli and O. A. Peverini, “UAV-Based Antenna Measurements: Improvement of the Test Source Frequency Behavior,” *IEEE Conference on Antenna Measurements & Applications (CAMA)*, Vasteras, 2018, pp. 1-3. doi: 10.1109/CAMA.2018.8530506

15. F. Paonessa, G. Virone, P. Bolli and A. M. Lingua, “UAV-based antenna measurements: Scan strategies,” 11th European Conference on Antennas and Propagation (EuCAP), Paris, 2017, pp. 1303-1305. doi: 10.23919/EuCAP.2017.7928721

16. P. Nepa and A. Buffi, “Near-Field-Focused Microwave Antennas: Near-field shaping and implementation,” in *IEEE Antennas and Propagation Magazine*, vol. 59, no. 3, pp. 42-53, June 2017. doi: 10.1109/MAP.2017.2686118